КРАТКИЕ СООБЩЕНИЯ

UDC 541.6:546.9:546.23:546.13

ELECTRONIC STRUCTURE AND MOLECULAR PROPERTIES OF $[Re_{6–x}Os_xSe_8Cl_6]^{(4–x)–}$ ($x = 0$—3) CLUSTERS: A STUDY BASED ON TIME-DEPENDENT DENSITY FUNCTIONAL THEORY INCLUDING SPIN-ORBIT AND SOLVENT EFFECTS

L. Alvarado-Soto, R. Ramirez-Tagle

Laboratorio de Bionanotechnologia, Universidad Bernardo O'Higgins, General Gana 1780, Santiago, Chile
E-mail: ramirez@ubo.cl

Relativistic time-dependent density functional (TDDFT) calculations including spin-orbit interactions via the zero order regular approximation (ZORA) and solvent effects are carried out on the $[Re_{6–x}Os_xSe_8Cl_6]^{(4–x)–}$ ($x = 0$—3) cluster. These calculations indicate that the lowest energy electronic transitions of the MMCT and LMCT type are similar to those observed in strongly luminescent 24-electron hexanuclear rhenium chalcogenide clusters $[Re_6Se_8Cl_6]^{4–}$. Thus our calculations predict that $[Re_{6–x}Os_xSe_8Cl_6]^{(4–x)–}$ ($x = 0$—3) clusters could be luminescent.

K e y w o r d s: luminescent cluster TTDFT.

The development of metal cluster-based inorganic and hybrid materials of technological interest calls for an understanding of their electronic structure, spectroscopy, photophysical and structural properties [1—5]. A remarkable class of molecular forms of inorganic clusters is the luminescent series M_6X_{12} (M = Mo, W; X = Cl, Br, I) and $Re_6Q_8L_6$ (Q = S, Se; L = halides, cyanide, phosphine, isothiocyanate, etc.), which exhibit rich photophysics with large quantum yields and significant microsecond emission lifetimes [1—19]. Also, both terminal and capping ligands induce a modulated dependence on the luminescence quantum yield [13—18]. Of particular note is the characteristic temperature dependent emission spectra and lifetimes observed in the series $[Re_6S_8X_6]^{4–}$ (X = Cl, Br, I) and thoroughly investigated by Kitamura *et al.* [20]. All these clusters are chemically stable under a variety of conditions, and they undergo facile ground-and-excited state electron-transfer reactions thereby representing an interesting class of metal cluster photoreceptors for chemical reactions induced by light [1—19]. A fiber optical oxygen sensor for power plant applications have been developed exploiting the observed efficient quenching by $_3O^2$ of the emission of red luminescence from the excited state of $[Mo_6Cl_8Cl_6]^{2–}$, which increases with decreasing oxygen concentration [6—8].

Among the large variety of octahedral metal chalcogenide clusters there are few phases containing mixed-metal cluster cores, such as $Mo_{6–x}M_xQ_8$, M = Re, Ru, Rh; Q = S, Se, Te [21—23]; the synthesis and crystal structure of new soluble heterometal Re—Mo and Re—Os cluster complexes is described [24—26].

Due to the structural similarity and isoelectronic nature with the above mentioned clusters, here we report the calculated optical properties of the $[Re_{6–x}Os_xSe_8Cl_6]^{(4–x)–}$ ($x = 0$—3) clusters.

Computational details. Our calculations for $[Re_{6–x}Os_xSe_8Cl_6]^{(4–x)–}$ ($x = 0$—3) were carried out using the Amsterdam density functional (ADF) code [27]. The spin-orbit relativistic effects were incorporated using the zero order regular approximation (ZORA) [27—29]. All the molecular structures were fully optimized via the analytical energy gradient method implemented by Verluis and Ziegler,
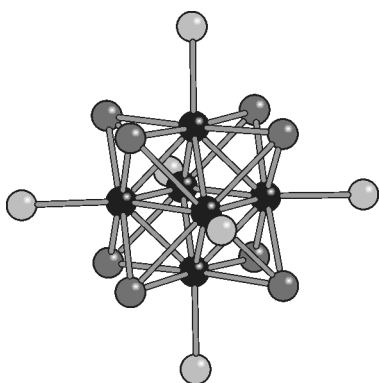
Fig. 1. Structure of the $[Re_{6-x}Os_xSe_8Cl_6]^{(4-x)-}$ ($x = 1$—3) cluster

which employs the local density approximation (LDA) within the Vosko—Wilk—Nusair parametrization for local exchange correlations [30, 31]. We also used the GGA (generalized gradient approximation) PW91 (Perdew-Wang) functional [32]. The excitation energies were estimated by spin-orbit time-dependent perturbation density functional theory (TDDFT) [33, 34]. Solvation effects were modeled by a conductor-like screening model for real solvents (COSMO) [35, 36] using acetonitrile as a solvent. The cluster geometry optimization and the excitations energies were calculated using the standard Slater-type-orbital (STO) basis sets with triple-zeta quality double plus polarization functions (TZ2P) for all atoms. We carried out harmonic frequency calculations on each cluster to confirm that the converged geometries were equilibrium structures.

Results and discussion. All these clusters were synthesized more than a decade ago [25] and since then there were no further studies reported on these clusters. Due to the lack of spectroscopic studies we undertook the task of studying the electronic structures and optical properties of these clusters using one the computational methods available (ADF) [27]. About a decade ago Arratia-Perez *et al.* successfully predicted the luminescence of 24*e* hexarhenium $[Re_6Q_8X_6]^{4-}$ clusters [9, 10], which were corroborated soon after [13—20], and recently we have studied the biological properties of the $[Re_6Se_8I_6]^{3-}$ cluster, particularity with the antitumoral and biomarker agent [37]. These $[Re_{6-x}Os_xSe_8Cl_6]^{(4-x)-}$ ($x = 0$—3) cluster ions exhibit a singlet ground state and are therefore diamagnetic. The calculated composition, location, and ordering of the occupied and unoccupied molecular orbitals of each cluster are very much alike. The lowest closely spaced manifold of unoccupied molecular orbitals indicates that these are mainly centered on the $[Re_{6-x}Os_x]$ core (Fig. 2) while the highest molecular orbitals (HOMOs) of all the cluster ions are mainly centered on the apical and bridge ligands (Fig. 3). Since there are not yet reported measurements of the electronic spectra of these $[Re_{6-x}Os_xSe_8Cl_6]^{(4-x)-}$ ($x = 0$—3) clusters, our results reported here may have a predictive character. The calculated allowed electronic transitions are summarized in Table 1. Also, all the contributions to these maximum intensities are assigned as LMCT (ligand-to-metal charge transfer) and MMCT (metal-to-metal charge transfer) type, and are similar if not identical to those observed in the isoelectronic and strongly luminescent $[Re_6Q_8X_6]^{4-}$ cluster series [6—10, 38]. The active molecular orbitals involved in these higher intensity transitions in each cluster correspond to HOMO, HOMO-1, HOMO-2, and HOMO-3 and the unoccupied molecular orbital LUMO+1, LUMO+2, and LUMO+4 for each cluster. The relative energy differences between the corresponding *cis—trans* and *fac—mer* isomers are 0.26 and 0.23 less stable respectively (Table 1). All the LUMOs are metallic, and in the heterometallic clusters the metal character in each HOMO is shared between the Re and Os atoms. The most stable structure for the $[Re_5OsSe_8Cl_6]^{3-}$ cluster corresponds to C_{4v} symmetry.

The frontier orbitals for each cluster are similar, with slight perturbations as a result of osmium incorporation; however, their close energy grouping allows even these small perturbations to alter the orbital ordering and LUMOs that are metal-metal antibonding in character (Fig. 2).

Conclusions. The electronic structure of these clusters indicates that their HOMOs are largely Cl based and the lowest excited states are closely spaced are largely centered on the cubic $[Re_{6-x}Os_x]$ core. The excitation energies of $[Re_{6-x}Os_xSe_8Cl_6]^{(4-x)-}$ ($x = 0$—3) clusters calculated using spin orbit time-dependent perturbation density functional theory (TDDFT) indicate that the most intense lowest energy transitions are of the LMCT and MMLC type with nonzero oscillator strengths. These results and the similarities with the strongly luminescent $[Re_6Se_8Cl_6]^{4-}$ cluster suggest that these anions could be luminescent.

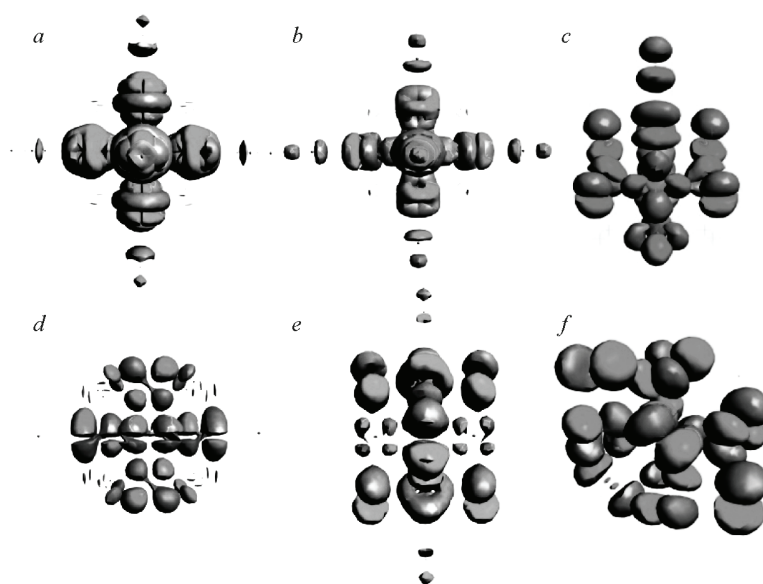*Fig. 2.* Active LUMOs involved in the higher intensity transitions in: (*a*) $Re_6Se_8Cl_6^{4-}$ [LUMO+3]; (*b*) $Re_5OsSe_8Cl_6^{3-}$ [LUMO+4]; (*c*) $Re_4Os_2Se_8Cl_6^{2-}$-*cis* [LUMO+1]; (*d*) $Re_4Os_2Se_8Cl_6^{2-}$-*trans* [LUMO+1]; (*e*) $Re_3Os_3Se_8Cl_6^{-}$-*mer* [LUMO+1]; (*f*) $Re_3Os_3Se_8Cl_6^{-}$-*fac* [LUMO+2]

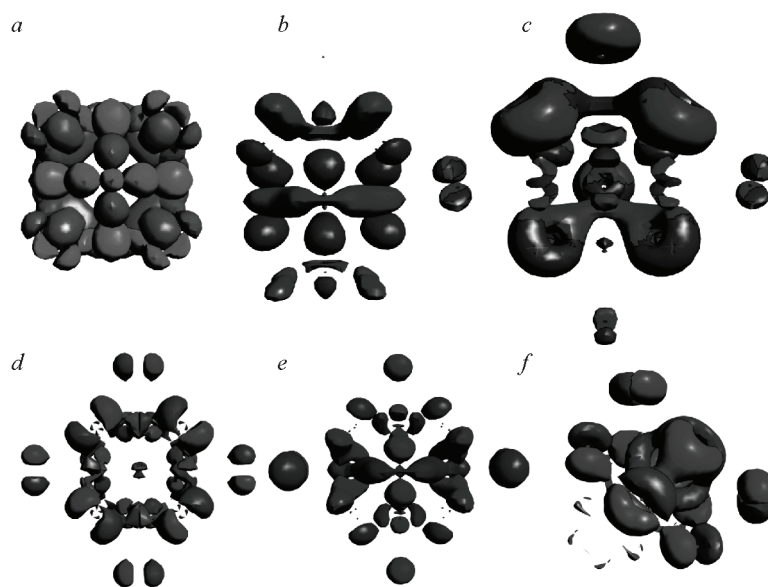*Fig. 3.* Active HOMOs involved in the higher intensity transitions in: (*a*) $Re_6Se_8Cl_6^{4-}$ [HOMO]; (*b*) $Re_5OsSe_8Cl_6^{3-}$ [HOMO-1]; (*c*) $Re_4Os_2Se_8Cl_6^{2-}$-*cis* [HOMO-3]; (*d*) $Re_4Os_2Se_8Cl_6^{2-}$-*trans* [HOMO-1]; (*e*) $Re_3Os_3Se_8Cl_6^{-}$-*mer* [HOMO-2]; (*f*) $Re_3Os_3Se_8Cl_6^{-}$-*fac* [HOMO]

T a b l e   1

TD-DFT+SO *Excitations energies calculated in a continuum solvation model and the relative bond energy*

Cluster	λ_{max}	Type [Percent composition of Re—Os—Se—Cl molecular active orbitals]	f^{a}	Relative bond energy, eV [b]
$Re_6Se_8Cl_6^{4-}$	619 MMCT	$68U_{3/2g} \rightarrow 69U_{3/2u}$ (HOMO) $\rightarrow$ (LUMO+3) [67-0-33-0] [61-0-26-13]	0.0022	0.0
$Re_5OsSe_8Cl_6^{3-}$	470 MMCT	$218E_{1/2} \rightarrow 221E_{1/2}$ (HOMO-1) $\rightarrow$ (LUMO+4) [64-5-32-0] [45-23-22-9]	0.0010	4.06
$Re_4Os_2Se_8Cl_6^{2-}$-*cis*	570 LMCT	$411E_{1/2} \rightarrow 416E_{1/2}$ (HOMO-3) $\rightarrow$ (LUMO+1) [12-0-65-26] [28-40-19-12]	00003	9.05
$Re_4Os_2Se_8Cl_6^{2-}$-*trans*	510 LMCT	$108E_{1/2g} \rightarrow 110E_{1/2u}$ (HOMO-1) $\rightarrow$ (LUMO+1) [9-0-65-26] [11-46-27-15]	0.0010	8.79
$Re_3Os_3Se_8Cl_6^{-}$-*mer*	620 LMCT	$412E_{1/2} \rightarrow 416E_{1/2}$ (HOMO-2) $\rightarrow$ (LUMO+1) [6-1-53-39] [7-60-25-7]	0.0006	14.60
$Re_3Os_3Se_8Cl_6^{-}$-*fac*	620 LMCT	$278E_{1/2} \rightarrow 281E_{1/2}$ (HOMO) $\rightarrow$ (LUMO+2) [12-1-56-31] [41-25-19-4]	0.0004	14.83

[a] Oscillator strength.

[b] Calculated using the PW91 functional and the lowest bond energy (–137.30 eV) as the reference value.

REFERENCES

1. *Gray H.B., Maverick A.W.* // Science. – 1981. – **214**. – P. 1201.
2. *Maverick A.W., Gray H.B.* // J. Amer. Chem. Soc. – 1981. – **103**. – P. 1298.
3. *Maverick A.W., Najdzionek J.S., Mackenzle D., Nocera D.G., Gray H.B.* // J. Amer. Chem. Soc. – 1983. – **105**. – P. 1878.
4. *Zietlow T.C., Hopkins M.D., Gray H.B.* // Inorg. Chem. – 1985. – **57**. – P. 112.
5. *Saito Y., Tanaka H.K., Sasaki Y., Azumi T.* // J. Phys. Chem. – 1985. – **89**. – P. 4413.
6. *Jackson J.A., Turro C., Newsham M.D., Nocera D.G.* // J. Phys. Chem. – 1990. – **94**. – P. 4500.
7. *Jackson J.A., Newsham M.D., Worsham C., Nocera D.* // Chem. Mater. – 1996. – **8**. – P. 558.
8. *Ghosh R.N., Baker G.L., Ruud C., Nocera D.G.* // Appl. Phys. Lett. – 1999. – **75**. – P. 2885.
9. *Arratia-Perez R., Hernandez-Acevedo L.* // J. Chem. Phys. – 1999. – **110**. – P. 2529.
10. *Arratia-Perez R., Hernandez-Acevedo L.* // J. Chem. Phys. – 1999. – **111**. – P. 168.
11. *Arratia-Perez R., Hernandez-Acevedo L.* // J. Chem. Phys. – 2003. – **118**. – P. 7425.
12. *Hernandez-Acevedo L., Arratia-Perez R.* // J. Chil. Chem. Soc. – 2003. – **48**. – P. 125.
13. *Yoshimura T., Ishizaka S., Umakoshi K., Sasaki Y., Kim H.B., Kitamura N.* // Chem. Lett. – 1999. – P. 697.
14. *Yoshimura T., Chen Z., Itasaka A., Abe M., Sasaki Y., Ishizaka S., Kitamura N.* // Inorg. Chem. – 2003. – **42**. – P. 4857.
15. *Kobayashi N., Ishizaka S., Yoshimura T., Kim H.-B., Sasaki Y., Kitamura N.* // Chem. Lett. – 2000. – P. 234.
16. *Yoshimura T., Ishizaka S., Kim H.-B., Kitamura N., Naumov N.G., Sokolov M., Fedorov E.V.* // Chem. Lett. – 1999. – P. 1121.

17. *Guilbaud C., Deluzet A., Domercq B., Molicie P., Coulon C., Boubekeur K., Batail P.* // J. Chem. Soc. Chem. Commun. – 1999. – P. 1867.
18. *Gray T.G., Rudzinski C.M., Nocera D.G., Holm R.H.* // Inorg. Chem. – 1999. – **38**. – P. 5932.
19. *Gabriel J.P., Boubekeur K., Uriel S., Batail P.* // Chem. Rev. – 2001. – **101**. – P. 2037.
20. *Kitamura N., Ueda Y., Ishizaka S., Yamada K., Aniya M., Sasaki Y.* // Inorg. Chem. – 2005. – **44**. – P. 6308.
21. *Berry F.J., Gibbs C.D., Greaves C.* // J. Solid State Chem. – 1991. – **92**. – P. 148.
22. *Honle W., Flack H.D., Yvon K.* // J. Solid State Chem. – 1983. – **43**. – P. 157.
23. *Perrin A., Chevrel R., Sergent M., Fischer O.* // J. Solid State Chem. – 1980. – **33**. – P. 157.
24. *Naumov N.G., Brylev K.A., Mironov Y.V., Virovets A.V., Fenske D., Fedorov V.E.* // Polyhedron. – 2003. – **23**. – P. 599.
25. *Tulsky E.G., Long J.R.* // Inorg. Chem. – 2001. – **40**. – P. 6990.
26. *Ramirez-Tagle R., Arratia-Perez R.* // J Clust Sci – 2009. – **20**. – P. 159.
27. Amsterdam Density Functional (ADF) Code, Release 2007, Vrije Universiteit, Amsterdam, The Netherlands.
28. *Van Lenthe E., Baerends E.J., Snijders G.* // J. Chem. Phys. – 1994. – **101**. – P. 9783.
29. *Te Velde G., Bickelhaupt F.M., Van Gisberger S.J.A., Fonseca Guerra C., Baerends E.J., Snijders J.G., Ziegler T.J.* // Comput. Chem. – 2001. – **22**. – P. 931.
30. *Verluis L., Ziegler T.* // J. Chem. Phys. – 1988. – **88**. – P. 322.
31. *Vosko S.H., Wilk L., Nusair M.* // Canad. J. Phys. – 1980. – **58**. – P. 1200.
32. *Perdew J.P., Wang Y.* // Phys. Rev. B. – 1992. – **13**. – P. 244.
33. *Runge E., Gross E.K.U.* // Phys. Rev. Lett. – 1984. – **52**. – P. 997.
34. *Wang F., Ziegler T., van Lenthe E., van Gisbergen S., Baerends E.J.* // J. Chem. Phys. – 2005. – **122**. – P. 204103.
35. *Klamt A., Jonas V.* // J. Chem. Phys. – 1996. – **105**. – P. 9972.
36. *Klamt A.* // J. Phys. Chem. – 1995. – **99**. – P. 2224.
37. *Echeverrıa C., Becerra A., Nunez-Villena F., Munoz-Castro A., Stehberg J., Zheng Z., Arratia-Perez R., Simon F., Ramırez-Tagle R.* // New J. Chem. – 2012. – **36**. – P. 927.
38. *Ramirez-Tagle R., Alvarado-Soto L., Hernández-Acevedo L., Arratia-Pérez R.* // J. Chil. Chem Soc. – 2010. – **54**. – P. 331.